

# Solar PV Integrated MPPT Controlled High Gain DC-DC Converter

Kalyani R. Lokhande

Department of Electrical Engineering  
NIT Warangal  
Warangal, India  
kr22eem1r11@student.nitw.ac.in

P.Raviteja

Department of Electrical Engineering  
NIT Warangal  
Warangal, India  
pr22eer1r08@student.nitw.ac.in

Narasimharaju B.L.

Department of Electrical Engineering  
NIT Warangal  
Warangal, India  
blnraju@nitw.ac.in

**Abstract**—This paper presents the integration of solar panels into standalone applications using a high-gain DC-DC converter coupled with an MPPT (Maximum Power Point Tracking) controller. Specifically, a Non-isolated Interleaved Quadratic Boost Converter topology serves as the DC-DC converter for the charge controller implementation. The Perturb and Observe method is the MPPT algorithm used, and it tracks the solar panel's maximum power. An interleaved quadratic boost converter raises the voltage while the photovoltaic array collects solar radiation and produces electricity. The performance of a high-gain converter, designed with specifications for 600W, 16/400V, and a 40KHz switching frequency, is validated through simulation using MATLAB SIMULINK, achieving an efficiency of 94.53%.

**Index Terms**—Non-Isolated Converter, High-Gain, DC-DC Converter, Solar Panel, PV Array Standalone Applications.

## I. INTRODUCTION

The escalating power consumption and rapid expansion of generation capacity are insufficient to meet industrial and commercial demands. Addressing this shortfall requires prioritizing the development of renewable energy sources to mitigate environmental pollution from fossil fuel depletion. However, variability in output from PV cells and wind mills due to climatic conditions presents a significant challenge. Consequently, strategies must be devised to stabilize output and ensure consistent energy provision.

The clean and renewable nature of solar energy makes it a very good substitute for traditional energy sources. As a result, installed solar photovoltaic systems have seen a sharp increase in capacity recently. Sunlight photovoltaic systems face a major difficulty from shading; even a 10% shade can result in a huge 30% loss of electricity overall, as shown in [1]. In response to this challenge, several solutions have been proposed in the existing literature.

Solar panels, comprised of solar cells, which are also referred to as photovoltaic cells, are devices designed to convert light into electricity, as mentioned in reference [2]. Typically, a 1-inch solar cell generates 1 watt of power. Multiple solar cells are connected in series and parallel to form a panel of a defined size, referred to as a PV module, to enhance power generation. These modules are further connected in series and parallel configurations, termed as PV arrays [3], to achieve specific currents and voltages.

There are several alternatives available for combining solar panels with DC-DC converters: series connection, parallel connection, or a mix of both. Opting for parallel connection can mitigate issues such as partial shading and voltage mismatch among parallel strings, resulting in the use of fewer blocking diodes, as mentioned in [4]. However, utilizing the maximum number of converters in a parallel topology may lead to low voltage at the input side. To overcome this limitation and achieve higher voltage at the output side, the utilization of high gain converters becomes necessary.

## II. LITERATURE SURVEY

Conventional boost converters have been used in recent years to increase voltage, but they have several drawbacks, including high stress across the switch, which forces large duty ratios to be chosen for the desired high voltage, which seriously impairs reverse recovery and introduces anomalous voltage spikes and conduction losses [5]. Quadratic boost converters are frequently employed in solar applications because they provide voltage stress equivalent to the output voltage, but they also increase the size and expense of the converter [6]. They achieve this by cascading two boost converters and using linked inductor techniques.

Alternatively, converters employing voltage multiplier cells, although reducing voltage stress due to the zero-voltage switching (ZVS) technique and boasting greater efficiency, become complex with the presence of transformers [7]. Transformerless DC-DC converters with two switches can only convert voltages between four and six times the input voltage; yet, they exhibit lower voltage stress than the output voltage [8]. As a result, these converters might not offer enough power for photovoltaic applications. While attempting to attain maximum performance within their individual restrictions through various ways, each topology offers distinct advantages.

In Section III of the study, the converter employed in solar applications is fully described electrically. Section IV shifts the focus to the details of the design and steady-state analysis. Section V presents the PV module's modeling. Section VI discusses the control techniques required to achieve and maintain a consistent output. The comprehensive simulation findings for the 600W prototype are covered in Section VII. Section VIII provides a conclusion to the study's findings.

### III. CIRCUIT DESCRIPTION

The paper referenced [9] utilizes a Converter for analyzing the MPPT strategy. Fig. 1 shows the power circuit of the high gain IQBC. A CBC structure is comprised of  $L_1$ ,  $D_1$ ,  $D_2$ , and  $D_2$ - $S_1$  within the IQBC. Similarly,  $L_3$ ,  $D_3$ ,  $D_4$ - $S_2$ , and  $C_2$  form another CBC structure.  $C_1$  and  $C_2$  serve as sources for  $L_2$ - $S_1$  and  $L_4$ - $S_2$ , respectively. With the first Conventional Boost Converter (CBC) structure acting as a source for the next, a Quadratic Boost Converter (QBC) is achieved. These two QBC structures are interleaved to form an IQBC. The output from one QBC combines with the second through the voltage lift capacitor Clift and intermediate diode Dint. Additionally, Diode  $D_0$  functions as the classical output diode, and capacitor  $C_0$  serves as the output capacitor.

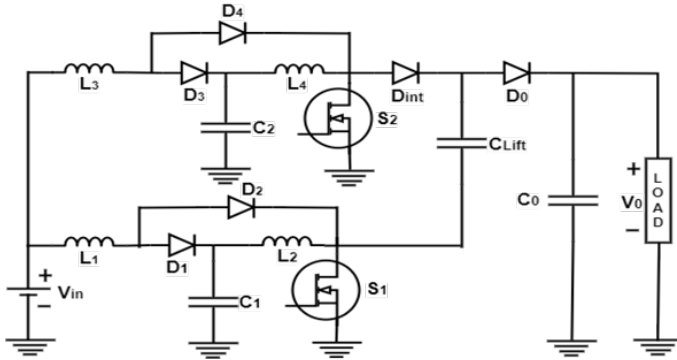


Fig. 1: Interleaved Quadratic Boost Converter [9]

### IV. STEADY STATE ANALYSIS AND DESIGN DETAILS

In this section, the paper presents expressions for designing the elements used in the high gain IQBC.

1) *Voltage Conversion Ratio*: The paper in reference [10] provides the equation for the voltage gain of the Quadratic Boost Converter (QBC), denoted by equation (1).

$$M = \frac{V_o}{V_{in}} = \frac{1}{(1-D)^2} \quad (1)$$

The variable D represents the duty ratio of the switch. In this converter, two Quadratic Boost Converter (QBC) structures are utilized, and their outputs are connected using Clift. Consequently, the Interleaved Quadratic Boost Converter (IQBC) yields a voltage gain as expressed in equation (2).

$$M = \frac{V_o}{V_{in}} = \frac{2}{(1-D)^2} \quad (2)$$

2) *Switches and Diodes Under Voltage Stress*: Equation (3) shows that in the high gain IQBC, the voltage stress on switches  $S_1$  and  $S_2$  is equal.

$$V_{S1} = V_{S2} = \frac{V_o}{2} \quad (3)$$

The voltage blocking capability of diodes  $D_1$  to  $D_4$  is described by equations (4) and (5).

$$V_{D1} = V_{D3} = \frac{V_o}{2}(1-D) \quad (4)$$

$$V_{D2} = V_{D4} = \frac{DV_o}{2} \quad (5)$$

During Mode 2, the output diode  $D_0$  is in a reverse bias state, as stated in [9]. Its voltage rating is determined through Kirchhoff's Voltage Law (KVL) and provided by equation (6).

$$V_{D0} = \frac{1}{(1-D)^2} V_{in} \quad (6)$$

3) *Current Stress on Semiconductor Devices*: When switches are in the ON state, the current stress on them is computed. Equations (7) and (8) are used to express the current stress on  $S_1$  and  $S_2$ .

$$I_{S1} = I_{L1} + I_{L2} \quad (7)$$

$$I_{S2} = I_{L3} + I_{L4} \quad (8)$$

Since diodes  $D_1$ - $D_4$  are positioned near the input port, their current carrying capacity is specified in equation (9).

$$I_{Dx} = \frac{I_{in}}{2}, x = 1, 2, 3, 4 \quad (9)$$

The current diode stress  $D_0$  is equivalent to the output current and is provided by equation (10).

$$I_{D0} = I_0 \quad (10)$$

4) *Design of Passive Components*: Equations (11) and (12) are the inductors design equations, which are obtained from the fundamental expression.

$$L_1 = L_3 = \frac{V_{in}D}{2f\Delta i_{in}} \quad (11)$$

$$L_2 = \frac{V_{C1}D}{f\Delta i_{L2}} \text{ and } L_4 = \frac{V_{C2}D}{f\Delta i_{L4}} \quad (12)$$

where  $\Delta i_{in}$  and  $\Delta i_{Lx}$  denote the input and inductor ripple current magnitudes, respectively, and f is the operation frequency. The voltage ripple and charging current that pass through capacitors are used to calculate their values. Equations (13) and (14) are utilized to obtain the capacitor values.

$$C_x = \frac{2I_0D}{(1-D)(f\Delta v_{C_x})}, x = 1, 2 \quad (13)$$

$$C_0 = \frac{I_0D}{f\Delta v_{C_0}} \quad (14)$$

## V. MODELLING OF PV MODULE

1) *Equivalent Circuit*: A p-n junction diode, usually composed of silicon, is the fundamental component of a solar cell. A parallel diode and a current source make up its fundamental components. The photovoltaic energy from the sun's rays, which excite the free electrons in the semiconductor and elevate their energy level, is what allows sunlight to illuminate the cell. Because current flow is made feasible as a result, solar energy can be turned straight into electrical energy without the need for further conversion processes. PV modules are made up of solar cells that are coupled in either parallel or series configurations to produce the necessary output. The analogous circuit of a solar PV cell is shown in Figure 2. Given is the result of the current  $I$ :

$$I = I_{ph} - I_D - I_{sh} \quad (15)$$

PV cells, which are the basic building blocks of PV modules, are linked together to create PV arrays using a series-parallel architecture. The fundamental formulas that control semiconductor and photovoltaic theory [4] include the PV cell's V-I characteristic, as explained below:

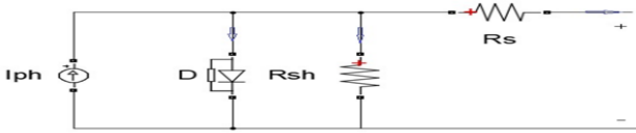


Fig. 2: Equivalent Circuit of a solar PV Cell

Essential elements that reflect a solar PV cell's electrical behavior make up its corresponding circuit. It consists of a current source ( $I_{ph}$ ) reflecting the generated photocurrent, a diode (D) representing the photovoltaic effect, a series resistance ( $R_s$ ) accounting for the inherent resistance of the semiconductor material, and a shunt resistance ( $R_{sh}$ ) representing the leakage current around the diode. This circuit is vital for understanding the solar cell's performance under different conditions, such as varying illumination levels and temperatures.

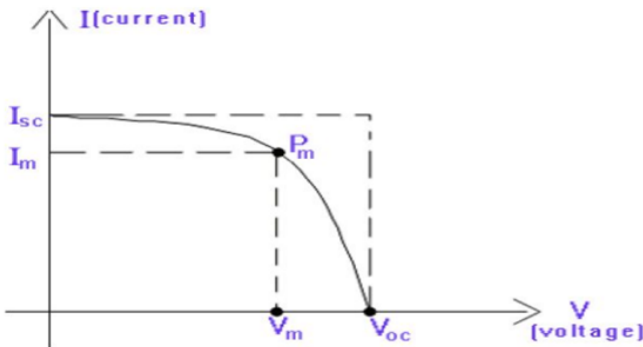


Fig. 3: Characteristics of a solar PV Cell

## VI. CONTROL SCHEME

Ensuring the match between the source and load is crucial for boosting efficiency in solar energy systems. However, the inherent low efficiency of solar cells poses a challenge. To address this, various methods are employed, among which Maximum Power Point Tracking (MPPT) stands out as highly effective. MPPT enables the capture of the maximum available power from solar cells. This paper discusses MPPT techniques, particularly focusing on closed-loop control systems. A Proportional-Integral (PI) controller is used to create closed-loop control, while the MPPT method makes use of the Perturb and Observe algorithm. The optimization of solar energy extraction efficiency is demonstrated by the practical implementation of MPPT with PI Controller on switches  $S_1$  and  $S_2$ .

1) *MPPT Algorithm*: Climate variations in temperature and radiation levels can cause oscillations in solar photovoltaic systems' output power. To maximize the power extracted from PV modules, the employment of Maximum Power Point Tracking (MPPT) algorithms is essential. These algorithms make it possible to extract the PV module's maximum power and make it easier for the load to receive it [4]. There are several MPPT techniques used, such as Fuzzy Logic, Open Circuit Voltage, and Perturb and Observe. The widely utilized Perturb and Observe approach, which is well-known for its simplicity and wide application, is often used for validation due to its ease of implementation.

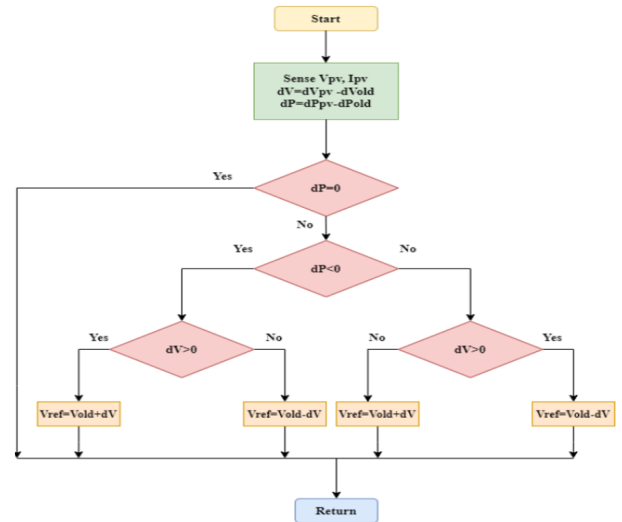


Fig. 4: Perturb and Observe Flowchart

2) *Closed Loop Control*: MPPT with closed-loop control is implemented for switches  $S_1$  and  $S_2$  in the system. The integral term ( $K_i$ ) is set to 0.121 and the proportional term ( $K_p$ ) to 0.01 in the closed-loop control. In order to attain the intended output value in a steady-state condition, these parameters were selected. By appropriately tuning the proportional and integral terms, the MPPT system can effectively regulate the operation of switches  $S_1$  and  $S_2$  to maintain the desired output power level under varying environmental conditions.

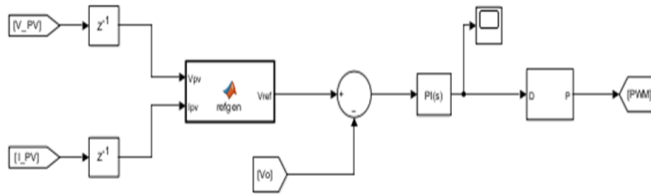


Fig. 5: The Perturb and Observe algorithm’s simulation diagram

### VII. SIMULATION RESULTS

An MPPT technique with closed-loop control is used to validate the simulation study of the converter [9]. To do this, a 600W simulation circuit is simulated with the parameters in Table I. The converter [9] has an input ripple current of 20% and an output voltage ripple of 10%. Plots of waveforms with varied reference values correspond to various temperatures and irradiances. Additionally, the switches duty ratio adjusts to temperature and irradiance changes. The requirements for the converter optimized for a 600W panel are listed in Table I [9], along with component ratings. This validation process ensures the accuracy and reliability of the MPPT algorithm with closed-loop control in optimizing the performance of the solar PV system.

TABLE I  
COMPONENT RATINGS

Parameters	Ratings(Unit)
Rated Power(Po)	600W
Input Voltage(Vi)	16V
Output Voltage(Vo)	400V
Duty Ratio(D)	0.75
Switching Frequency (fs)	40KHz
Inductor(L1/L2,L3/ L4)	200μH/1.5mH
Capacitor(C1,C2)	100 μF
Lift Capacitor (Clift)	4.7 μF
Capacitor(Co)	300μF
Resistor(Ro)	266.6ohm

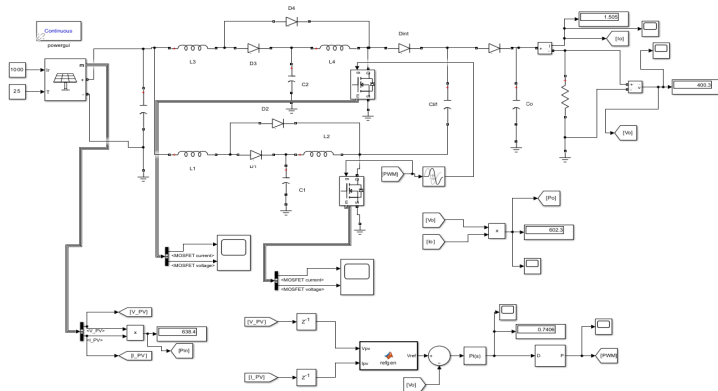


Fig. 6: Simulation Diagram

The simulation results depicted in Figures 7 to 9 illustrate the performance under conditions of 25°C temperature and 1000 W/m<sup>2</sup> irradiation, with a reference voltage set at 360V. Through adjusting the duty ratio, the system aims to achieve maximum output efficiency.

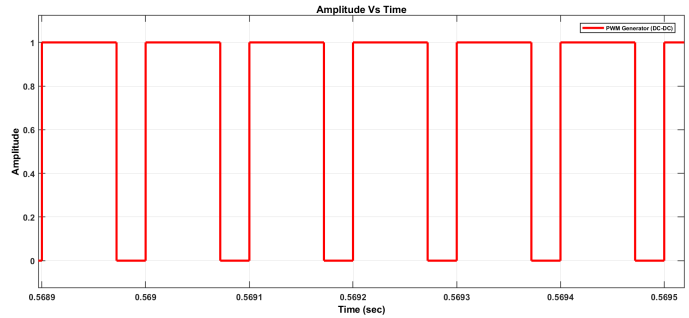


Fig. 7: Pulses to the gate

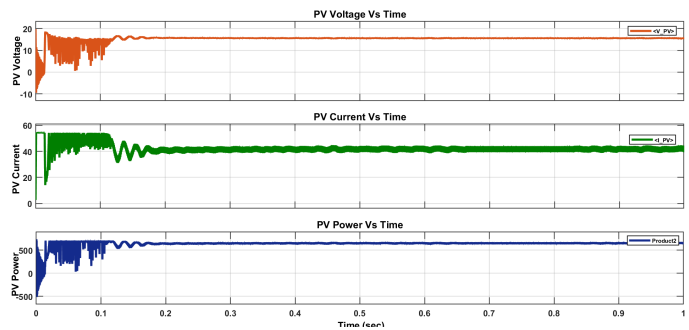


Fig. 8: PV Panel Outputs

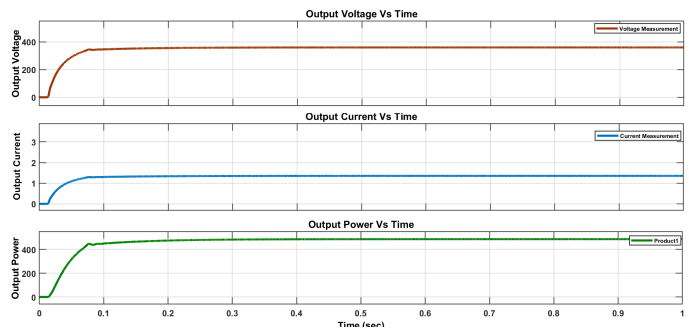


Fig. 9: Output Voltage, Current and Power

The system exhibits a 360V output voltage at a duty cycle of 0.7 and a switching frequency of 40kHz. Concurrently, an output current of 1.354A is observed, leading to a resultant output power of 488W. Figures 10 to 13 exhibit the simulation outcomes for conditions involving a temperature of 25°C and irradiation of 1000 W/m<sup>2</sup>, with a reference voltage set at 400V. The system maintains an output current of 1.5A and output power of 600W. The duty ratio is optimized to attain maximum output efficiency.

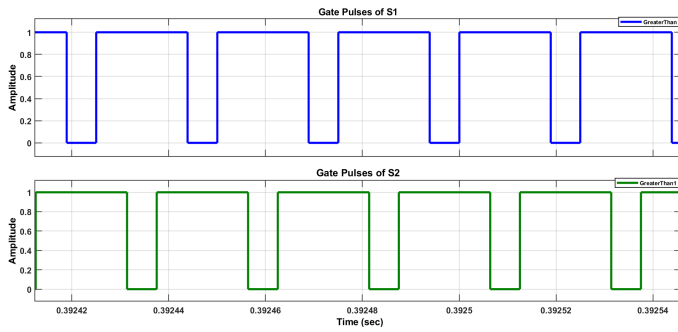


Fig. 10: Gate pulses of switch  $S_1$  and  $S_2$

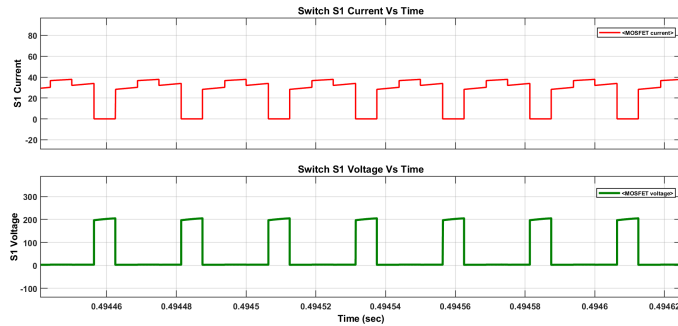


Fig. 11: Switch  $S_1$  Current and Voltage



Fig. 12: Switch  $S_2$  Current and Voltage

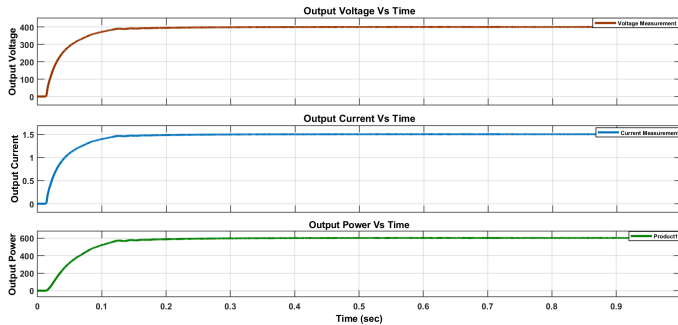


Fig. 13: Output Voltage, Current and Power

With a reference voltage set at 400V, the simulation results displayed in Fig. 14 demonstrate the performance under  $35^\circ\text{C}$  and  $1000\text{ W/m}^2$  irradiation conditions. The input voltage is

maintained at the maximum power point voltage of 16V in both cases. Temperature variations cause a small shift in the duty ratio, which the proportional-integral (PI) controller corrects by modifying the pulse width modulation (PWM) signals to bring the duty ratio closer to the reference value. Furthermore, closed-loop and MPPT control techniques guarantee that the output voltage stays at the reference voltage level.

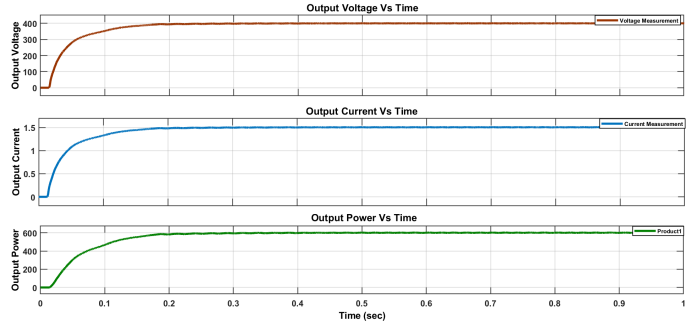


Fig. 14: Output Voltage, Current and Power  
When the input voltage is set to 18V, the system consistently maintains the output voltage at 400V, current at 1.5A, and power level at 600W, as illustrated in Figure 15.

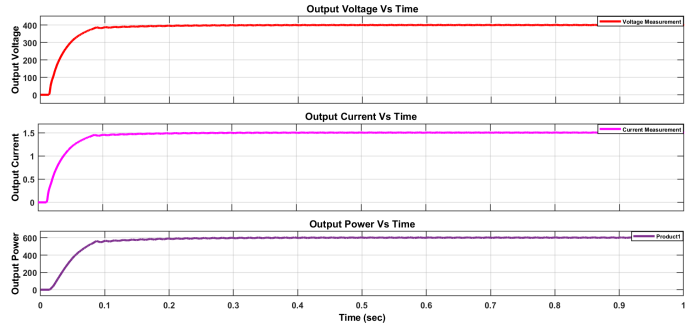


Fig. 15: Output Voltage, Current and Power

When transitioning from 16V to 18V, the system consistently maintains an output voltage of 400V, with both current and power levels remaining unchanged. This stability highlights the system's ability to preserve desired output parameters despite fluctuations in input voltage.

By altering the load resistance to 500 ohms, the system consistently maintains an output voltage of 400V, as illustrated in Figure 16.

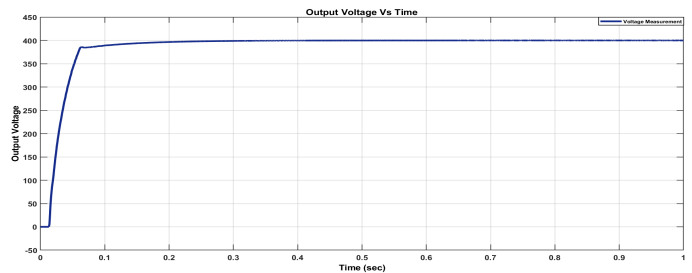


Fig. 16: Output Voltage

By adjusting the load resistance to 1000 ohms, the system consistently sustains an output voltage of 400V, as depicted in Figure 17.

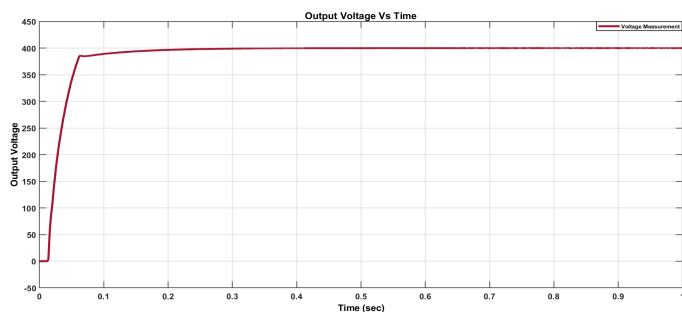


Fig. 17: Output Voltage

Indeed, the consistent output voltage of 400V despite variations in the load resistance demonstrates the stability of the system under different load conditions. This stability suggests that the system can effectively regulate the output voltage, ensuring reliable performance even when the load changes.

When evaluating the appropriateness of the chosen MPPT algorithm, Perturb and Observe (P&O), for the Solar PV Integrated MPPT Controlled non-isolated High Gain DC-DC Converter, it's crucial to explore alternative algorithms that might yield enhancements. While P&O is widely utilized due to its simplicity and efficacy, other MPPT algorithms offer distinct characteristics and potential advantages. For example, the Incremental Conductance (IncCond) algorithm adjusts the operating point by considering the incremental conductance of the PV array, potentially providing improved accuracy, especially under rapidly changing irradiance conditions.

The Fractional Open Circuit Voltage (FOCV) algorithm tracks the optimal operating point by utilizing the ratio of open-circuit voltage to maximum power point voltage, which can be particularly advantageous in systems with variable temperature conditions. Model Predictive Control (MPC) leverages dynamic models of the PV system to anticipate future behavior and determine optimal operating points, potentially enhancing performance in scenarios with partial shading or quickly changing weather conditions. Moreover, artificial intelligence-based algorithms, such as neural networks, fuzzy logic, or genetic algorithms, can be customized to specific system attributes and environmental variables, offering the potential for superior performance.

Investigating these alternative algorithms through comparative studies could yield insights into potential enhancements in the Solar PV Integrated MPPT Controlled non-isolated High Gain DC-DC Converter's performance, while considering factors such as implementation complexity, computational demands, and cost-effectiveness.

Within the domain of DC-DC converter topologies, the Non-isolated Interleaved Quadratic Boost Converter exhibits a range of distinct advantages, making it an attractive option across diverse applications. Its primary advantage lies in its superior efficiency, particularly evident under higher input

voltages and moderate-to-high loads. The interleaved design of this converter effectively minimizes switching losses, thereby enhancing overall efficiency levels.

Additionally, its capability to distribute input current ripple across multiple phases mitigates undesirable fluctuations, a crucial attribute for applications sensitive to such disturbances, such as renewable energy systems. Furthermore, the Non-isolated Interleaved Quadratic Boost Converter offers reduced electromagnetic interference (EMI) due to its distributed power dissipation, making it well-suited for applications requiring compliance with stringent EMI standards, such as automotive electronics or medical devices. Its inherent scalability facilitates straightforward adaptation to higher power demands by the addition of more phases, without unduly straining individual components. Moreover, the distributed heat dissipation inherent in the interleaved topology enhances thermal management, enabling the utilization of smaller and more effective cooling solutions.

Collectively, these benefits establish the Non-isolated Interleaved Quadratic Boost Converter as a versatile and resilient option suitable for various applications prioritizing efficiency, ripple control, EMI mitigation, scalability, thermal performance, and reliability.

## VIII. CONCLUSION

This work presents the MPPT with PI controller for closed loop control and tracking the maximum power, respectively. It has been demonstrated using MPPT that the load receives the maximum power supplied by the PV array for the specific irradiance levels. If there is a change in temperature, the same is done. The system is extremely efficient thanks to a straightforward MPPT configuration, and MATLAB is used to simulate the high gain converter. The converter can achieve a steady state value at the required output voltage by including a PI controller. As a result, applications requiring a steady DC output voltage can utilize the converter.

## REFERENCES

- [1] Masatoshi Uno, Yota Saito, Shinichi Urabe, and Masaya Yamamoto. Pwm switched capacitor-based cell-level power balancing converter utilizing diffusion capacitance of photovoltaic cells. *IEEE Transactions on Power Electronics*, 34(11):10675–10687, 2019.
- [2] Hamzah Eteruddin, Atmam Atmam, David Setiawan, and Yanuar Z Arief. Effects of the temperature on the output voltage of mono-crystalline and poly-crystalline solar panels. *Sinergi*, 24(1):73–80, 2020.
- [3] Ramesh Babu Kodati and Puli Nnageshwar Rao. A review of solar cell fundamentals and technologies. *Advanced Science letters*, 26, 2020.
- [4] HS Rauschenbach et al. Solar cell array design handbook, vol. 1. *Jet Propulsion Laboratory, California Institute of Technology, Pasadena, California*, 91103:490, 1976.
- [5] Y Zhao, W Li, Y Deng, and X He. High step-up boost converter with passive lossless clamp circuit for non-isolated high step-up applications. *IET power electronics*, 4(8):851–859, 2011.
- [6] Luiz Henrique Silva Colado Barreto, Ernane Antônio Alves Coelho, Valdeir José Farias, João Carlos de Oliveira, Luis Carlos de Freitas, and Jr Joao Batista Vieira. A quasi-resonant quadratic boost converter using a single resonant network. *IEEE Transactions on Industrial Electronics*, 52(2):552–557, 2005.
- [7] Yan Deng, Qiang Rong, Wuhua Li, Yi Zhao, Jianjiang Shi, and Xiangning He. Single-switch high step-up converters with built-in transformer voltage multiplier cell. *IEEE Transactions on Power Electronics*, 27(8):3557–3567, 2012.

- [8] Lung-Sheng Yang, Tsorng-Juu Liang, and Jiann-Fuh Chen. Transformerless dc-dc converters with high step-up voltage gain. *IEEE Transactions on Industrial Electronics*, 56(8):3144–3152, 2009.
- [9] Vijay Joseph Samuel, Gna Keerthi, and M Prabhakar. High gain interleaved quadratic boost dc/dc converter. In *2019 2nd International Conference on Power and Embedded Drive Control (ICPEDC)*, pages 390–395. IEEE, 2019.
- [10] K Tattiwong and C Bunlaksanusorn. Analysis design and experimental verification of a quadratic boost converter. In *TENCON 2014-2014 IEEE Region 10 Conference*, pages 1–6. IEEE, 2014.